Available online at www.sciencedirect.com

SCIENCE DIRECT®

Biochemical Pharmacology 70 (2005) 1796–1806

Biochemical Pharmacology

www.elsevier.com/locate/biochempharm

# Mitochondria-targeted peptide prevents mitochondrial depolarization and apoptosis induced by *tert*-butyl hydroperoxide in neuronal cell lines

Kesheng Zhao, Guoxiong Luo, Serena Giannelli, Hazel H. Szeto *

*Department of Pharmacology, Joan and Sanford I. Weill Medical College of Cornell University, 1300 York Avenue, New York, NY 10021, USA*

Received 5 July 2005; accepted 29 August 2005

## Abstract

Oxidative stress and mitochondrial oxidative damage have been implicated in aging and many common diseases. Mitochondria are a primary source of reactive oxygen species (ROS) in the cell, and are particularly susceptible to oxidative damage. Oxidative damage to mitochondria results in mitochondrial permeability transition (MPT), mitochondrial depolarization, further ROS production, swelling, and release of cytochrome *c* (cyt *c*). Cytosolic cyt *c* triggers apoptosis by activating the caspase cascade. In the present work, we examined the ability of a novel cell-penetrating, mitochondria-targeted peptide antioxidant in protecting against oxidant-induced mitochondrial dysfunction and apoptosis in two neuronal cell lines. Treatment with *tert*-butyl hydroperoxide (*t*BHP) for 24 h resulted in lipid peroxidation and significant cell death via apoptosis in both $N_2A$ and SH-SY5Y cells, with phosphatidylserine translocation, nuclear condensation and increased caspase activity. Cells treated with *t*BHP showed significant increase in intracellular ROS, mitochondrial depolarization and reduced mitochondrial viability. Concurrent treatment with <1 nM SS-31 (D-Arg-Dmt-Lys-Phe-$NH_2$; Dmt = 2′,6′-dimethyltyrosine) significantly decreased intracellular ROS, increased mitochondrial potential, and prevented *t*BHP-induced apoptosis. The remarkable potency of SS-31 can be explained by its extensive cellular uptake and selective partitioning into mitochondria. Intracellular concentrations of [$^3$H]SS-31 were 6-fold higher than extracellular concentrations. Studies using isolated mitochondria revealed that [$^3$H]SS-31 was concentrated ~5000-fold in the mitochondrial pellet. By concentrating in the inner mitochondrial membrane, SS-31 is localized to the site of ROS production, and can therefore protect against mitochondrial oxidative damage and further ROS production. SS-31 represents a novel platform of mitochondria-targeted antioxidants with broad therapeutic potential.


*Keywords:* Oxidative stress; Mitochondrial permeability transition; Reactive oxygen species; Antioxidant; Cell-penetrating cationic peptides

## 1. Introduction

Cellular oxidative injury is implicated in aging and a wide array of clinical disorders. Reactive oxygen species (ROS) can damage cells by oxidizing membrane phospholipids, proteins, and nucleic acids. These damaging effects of ROS are normally kept under control by endogenous antioxidant systems including glutathione, ascorbic acid, and enzymes such as superoxide dismutase, glutathione peroxidase, and catalase. Oxidative stress occurs when antioxidant systems are overwhelmed by ROS, and the resulting oxidative damage can lead to cell death.

*tert*-Butyl hydroperoxide (*t*BHP) is a membrane-permeant oxidant compound that can induce cell death via apoptosis or necrosis [1,2]. At low doses, *t*BHP causes apoptosis as demonstrated by DNA fragmentation and condensation of the nuclei. At higher doses, *t*BHP treatment results in the release of lactate dehydrogenase (LDH) and membrane blebbing. These are thought to be mediated by the generation of free radicals and lipid and protein peroxidation. Inside the cell, *t*BHP generates *tert*-butoxyl radicals via iron-dependent reactions similar to the Fenton reaction, resulting in lipid peroxidation, depletion of intracellular glutathione, followed by modification of protein thiols, and loss of cell viability [3–5]. In prooxidant-treated cells,

*Abbreviations:* cyt *c*, cytochrome *c*; DCF, dichlorofluorescein; Dmt, 2′,6′-dimethyltyrosine; 4-HNE, 4-hydroxynonenol; LDH, lactate dehydrogenase; MPT, mitochondrial permeability transition; ROS, reactive oxygen species; SS-31, D-Arg-Dmt-Lys-Phe-$NH_2$; *t*BHP, *tert*-butyl hydroperoxide; TMRM, tetramethylrhodamine methyl ester

* Corresponding author. Tel.: +1 212 746 6232; fax: +1 212 746 8835.
*E-mail address:* hhszeto@med.cornell.edu (H.H. Szeto).

0006-2952/$ – see front matter © 2005 Elsevier Inc. All rights reserved.
doi:10.1016/j.bcp.2005.08.022

there is also impairment of $Ca^{2+}$ transport and subsequent perturbation of intracellular $Ca^{2+}$ homeostasis, resulting in a sustained increase in cytosolic $Ca^{2+}$ concentration [6,7]. This increase in $Ca^{2+}$ can cause activation of various $Ca^{2+}$-dependent degradative enzymes which may contribute to cell death. However, in SH-SY5Y neuroblastoma cells treated with *t*BHP, cell death was associated with free radical production rather than increase in intracellular $Ca^{2+}$ [8].

Recent evidence suggest that *t*BHP-induced apoptosis is triggered by mitochondrial permeability transition (MPT) accompanied by mitochondrial depolarization [9,10,2]. The MPT pore is a high-conductance channel that is believed to be form by the apposition of the voltage-dependent anion channel on the outer mitochondrial membrane and the adenine nucleotide translocator on the inner membrane [11]. Opening of the MPT pore causes a sudden increase in permeability of the inner mitochondrial membrane. This results in dissipation of the mitochondrial potential, uncoupling of oxidative phosphorylation, swelling of the mitochondrial matrix, and rupture of the outer mitochondrial membrane [12,13]. The rupture of the outer mitochondrial membrane allows the release of cytochrome *c* (cyt *c*) into the cytosol where it induces activation of the caspase cascade responsible for apoptotis execution [14,15]. ROS may promote MPT by causing oxidation of thiol groups on the adenine nucleotide translocator [16–18]. In addition, cyt *c* is normally bound to the inner mitochondrial membrane by an association with cardiolipin, and peroxidation of cardiolipin induces the dissociation of cyt *c* into the intermembrane space [19].

These findings suggest that oxidative damage to mitochondria is a critical event in oxidative cell damage, and mitochondrial ROS should be a primary target for drug development [20,21]. Available antioxidants tend to be poorly cell-permeable and do not distribute well to mitochondria. Reduction in ROS production with the use of mitochondrial uncouplers has been proposed as a means to reduce mitochondrial ROS generation [22–24]. However, long-term use of uncouplers would have detrimental effects on ATP production. We recently discovered a series of small cell-penetrating peptide antioxidants that localize to the inner mitochondrial membrane [25]. SS-31 (D-Arg-Dmt-Lys-Phe-$NH_2$; Dmt = 2′,6′-dimethyltyrosine) is one peptide analog in this series that can scavenge ROS and inhibit lipid peroxidation in vitro. In addition, SS-31 can reduce mitochondrial ROS production, inhibit MPT, and prevent mitochondrial swelling in isolated mitochondria. Preliminary studies showed that SS-31 is very potent in protecting against *t*BHP-induced cell death [25]. In this study, our aim was to further investigate the ability of SS-31 to prevent *t*BHP-induced apoptosis in two neuronal cell lines, $N_2A$ and SH-SY5Y cells. We found that SS-31 is very potent ($EC_{50} < 1$ nM) in preventing *t*BHP-induced apoptosis, and this was associated with decreased ROS production and mitochondrial protection. A control non-scavenging peptide (SS-20; Phe-D-Arg-Phe-Lys-$NH_2$) [25], did not protect against *t*BHP-induced cytotoxicity. These findings support a role for ROS production and MPT in oxidant-induced apoptosis. We also determined that the remarkable potency of SS-31 is due to its extensive uptake into cells and partitioning into mitochondria.

## 2. Materials and methods

### 2.1. Drugs and chemicals

SS-31 and SS-20 were synthesized and provided by Dr. Peter W. Schiller (Clinical Research Institute of Montreal, Montreal, Quebec, Canada). [$^3$H]SS-31 was prepared by Dr. Geza Toth (Institute of Isotopes, Budapest, Hungary) using a previously described method [26]. All cell culture supplies and fluorescent probes were obtained from Invitrogen (Carlsbad, CA). Unless specified, all other reagents were supplied by Sigma–Aldrich, St. Louis, MO.

### 2.2. Cell culture

$N_2A$ cells were kindly provided by Dr. Gunnar Gouras (Department of Neurology, Weill Medical College of Cornell University, New York, NY). SH-SY5Y cells were obtained from the American Type Culture Collection (Manassas, VA). $N_2A$ cells were grown in 50% DMEM and 50% Opti-MEM containing 5% FBS, penicillin (100 units/ml) and streptomycin (0.1 mg/ml). SH-SY5Y cells were grown in DMEM containing 10% FBS, penicillin (100 units/ml) and streptomycin (0.1 mg/ml). Cells were cultured and maintained at 37 °C and 5% $CO_2$. Cells were trypsinized and subcultured every 2 days for $N_2A$ cells and every 4 days for SH-SY5Y cells.

### 2.3. Measurement of cell and mitochondrial viability

Cells were plated in 96-cell plates at a density of $1 \times 10^4$/well for $N_2A$ cells or $4 \times 10^4$/well for SH-SY5Y cells for 24 h. The cells were then incubated with *t*BHP alone, or in the presence of SS-31 or SS-20, for 24 h. Cell viability was evaluated by measuring lactate dehydrogenase (LDH) released from the cells using the Cytotoxicity Detection Kit (Roche Diagnostics GmbH, Mannheim, Germany). Mitochondrial function was determined by measuring NADPH dehydrogenase activity using the MTS assay (Promega, Madison, WI).

### 2.4. Detection of lipid peroxidation

4-Hydroxynonenol (4-HNE), one of the major aldehyde products of the peroxidation of membrane polyunsaturated fatty acids, was determined by immunofluorescence using an anti-HNE antibody. $N_2A$ cells were seeded on glass bottom dish (MatTek, Ashland, MA) 1 day before *t*BHP treatment (1 mM) for 3 h at 37 °C in the absence or presence of SS-31 ($10^{-12}$ to $10^{-9}$ M). Cells were fixed with 4% paraformaldehyde, permeabilized with a $CH_2OH$:$CH_3$-COOH (95:5) mixture, and incubated with a rabbit anti-HNE antibody (Calbiochem, San Diego, CA) for 2 h followed by goat anti-rabbit IgG conjugated to biotin for 30 min. Cells were then washed and incubated with avidin-FITC conjugate for 30 min, and mounted in Vectashield (Vector Laboratories Inc., Burlingame, CA) and imaged using a Zeiss fluorescence microscope (Axiovert 200M) equipped with the Apochromat 40× objective, using an excitation wavelength of 460 ± 20 nm and a longpass filter of 505 nm for emission.

### 2.5. Detection of apoptosis by Annexin V

$N_2A$ cells were treated with 50 μM of *t*BHP alone, or with 1 nM SS-31, at 37 °C for 6 h. Cells was washed twice and stained with Alexa fluor 488 Annexin V and propidium iodide (Vybrant Apoptosis Assay Kit #2) according to manufacturer's instructions, and imaged using a Zeiss fluorescent microscope as described above.

### 2.6. Detection of apoptosis by Hoechst staining

$N_2A$ and SH-SY5Y cells were grown on 96-well plates, treated with *t*BHP in the absence or presence of SS-31 ($10^{-12}$ to $10^{-8}$ M) at 37 °C for 12–24 h. All treatments were carried out in quadruplicates. Cells were then stained with 2 μg/ml Hoechst 33342 for 20 min, fixed with 4% paraformaldehyde, and imaged using a Zeiss fluorescent microscope as described above. Nuclear morphology was evaluated using an excitation wavelength of 350 ± 10 nm and a longpass filter of 400 nm for emission. All images were processed and analyzed using the MetaMorph software (Universal Imaging Corp., West Chester, PA). Uniformly stained nuclei were scored as healthy, viable neurons, while condensed or fragmented nuclei were scored as apoptotic.

### 2.7. Measurement of caspase activity

Caspase activity was assayed using a commercial kit based on fluorochrome-labeled caspase inhibitors (FLICA, Immunochemistry Technologies LLC, Bloomington, MN) [27]. $N_2A$ cells were treated with *t*BHP (50 μM, 12h, 37 °C, 5% $CO_2$) alone, or with different concentrations of SS-31 ($10^{-12}$ to $10^{-8}$ M). After treatment, cells were gently lifted from plates with a cell detachment solution (Accutase, Innovative Cell Technologies Inc., San Diego, CA) and washed twice in PBS. According to the manufacturer's recommendation, cells were resuspended (~$5 \times 10^6$ cells/ml) in PBS and labeled with pan-caspase inhibitor/marker FAM-VAD-FMK for 1 h at 37 °C under 5% $CO_2$ and protected from the light. Cells were then rinsed to remove the unbound reagent and fixed. Cell fluorescence was measured by a microplate spectrofluorometer (ex/em = 488/520 nm) (Molecular Devices, Sunnyvale, CA).

Caspase-9 activity was determined using the caspase-9 FLICA™ kit containing red fluorescent inhibitor SR-LEHD-FMK and Hoechst 33342 (Immunochemistry Technologies LLC, Bloomington, MN), according to manufacturer's instructions. Cells were imaged by fluorescence microscopy (ex/em = 560/590 nm for SR-FLICA and 365/480 nm for Hoechst).

### 2.8. Measurement of intracellular ROS

Intracellular ROS was evaluated using the fluorescent probe DCFDA (5-(and-6)-carboxy-2′,7′-dichlorodihydrofluorescein diacetate). For visualization by fluorescent microscopy, $N_2A$ cells were plated in glass bottom dishes and treated with 50 μM *t*BHP, alone or with SS-31, for 6 h. Cells were then washed and loaded with 10 μM of DCFDA for 30 min at 37 °C, and imaged by fluorescent microscopy (ex/em = 495/525 nm). For quantitative assessment of ROS production, $N_2A$ cells in 96-well plates were washed with HBSS and loaded with 10 μM of DCFDA for 30 min at 37 °C. Cells were washed three times with HBSS and exposed to 100 μM of *t*BHP, alone or with SS-31. The oxidation of DCF was monitored in real time by a microplate spectrofluorometer (Molecular Devices, Sunnyvale, CA) using ex/em wavelengths of 485/530 nm.

### 2.9. Measurement of mitochondrial membrane potential

Mitochondrial membrane potential was evaluated using the fluorescent probe TMRM (tetramethylrhodamine methyl ester). $N_2A$ cells were plated in glass bottom dishes and treated with 50 μM *t*BHP, alone or with SS-31, for 6 h. Cells were loaded with 20 nM of TMRM towards the last 20 min of incubation. Fluorescent microscopy was carried out as described above using ex/em wavelengths of 552/570 nm.

### 2.10. Measurement of cell uptake of SS-31

$N_2A$ cells ($2 \times 10^5$/well) were incubated with 0.3 ml of [$^3$H]SS-31 (20 nM) at 37 °C for 60 min, and radioactivity was determined in the medium and in cell lysate [28,25]. The reading in medium was subtracted from the reading obtained in cell lysate.

### 2.11. Measurement of mitochondrial uptake of SS-31

Mitochondrial uptake of SS-31 was determined using isolated mouse liver and rat brain mitochondria. Mouse liver mitochondria were prepared as described in our earlier paper [25]. Rat brain mitochondria were prepared according to the method by Sullivan et al. [29] with the exception that a discontinuous Percoll gradient was used instead of a Ficoll gradient. For uptake studies, liver mitochondria (100 μg) were incubated in 0.5 ml buffer

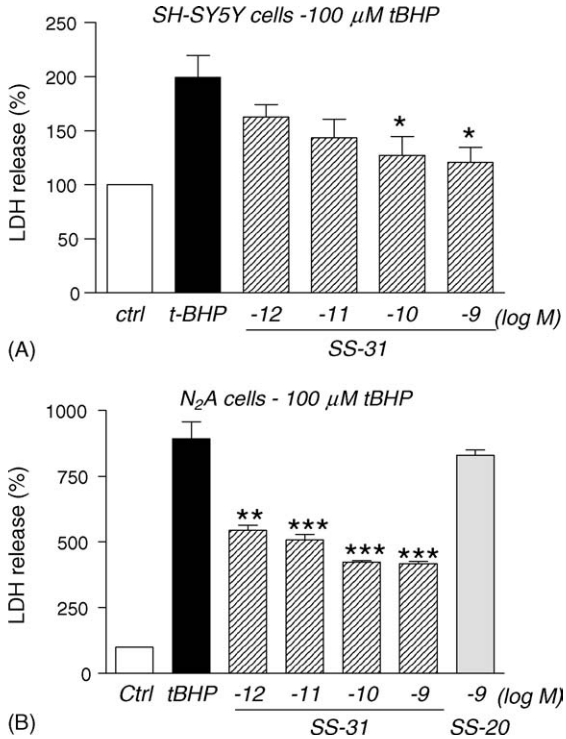


Fig. 1. SS-31 reduced *t*BHP-induced LDH release in SH-SY5Y (A) and $N_2A$ (B) cells. Cells were treated with 100 μM *t*BHP alone, or with SS-31, for 24 h. $^*P < 0.05$, $^{**}P < 0.01$, $^{***}P < 0.001$, compared to *t*BHP alone.

(70 mM sucrose, 230 mM mannitol, 3 mM Hepes, 5 mM succinate, 5 mM $KH_2PO_4$, 0.5 μM rotenone, pH 7.4) containing 1 μM SS-31 and [$^3$H]SS-31 for various times at RT and radioactivity was determined in the mitochondrial pellet [25]. Brain mitochondria (100 μg) were incubated in 0.4 ml buffer (75 mM sucrose, 215 mM mannitol, 20 mM Hepes, 5 mM glutamate, 0.5 mM malate, pH 7.2) containing 1 μM SS-31 and [$^3$H]SS-31 for 5 min at RT.

### *2.12. Data analysis*

All data are presented as mean ± S.E. Differences among groups were compared by ANOVA. Post hoc analyses were carried out using the Dunnett's test comparing peptide treatment with *t*BHP exposure alone.

## 3. Results

### *3.1. SS-31 protected SH-SY5Y and $N_2A$ cells against tBHP induced cytotoxicity*

The loss of cell viability induced by 100 μM *t*BHP was accompanied by a significant increase in LDH release in SH-SY5Y (Fig. 1A) and $N_2A$ cell (Fig. 1B). Concurrent treatment of cells with SS-31 resulted in dose-dependent decrease in LDH release in both SH-SY5Y ($P < 0.01$) and $N_2A$ cells ($P < 0.0001$). LDH release was reduced significantly by 0.1 and 1 nM of SS-31 in both cell lines ($P < 0.05$). SS-20, the control non-scavenging peptide, did not protect against *t*BHP-induced cytotoxicity in $N_2A$ cells (Fig. 1B).

### *3.2. SS-31 reduced tBHP-induced lipid peroxidation*

4-Hydroxy-2-nonenol (HNE), one of the major aldehyde products of the peroxidation of membrane polyunsaturated fatty acids, has been suggested to contribute to oxidant stress-mediated cell injury [30,31]. Fig. 2 shows that treatment of $N_2A$ cells with 1 mM *t*BHP for 3 h resulted in increased production of 4-HNE as determined by immunofluorescence using an anti-HNE antibody (panel b). Concurrent treatment with 10 nM SS-31 prevented 4-HNE accumulation caused by *t*BHP (panel c).

### *3.3. SS-31 protected against tBHP-induced apoptosis*

Our results suggest that *t*BHP induced apoptotic cell death in both $N_2A$ and SH-SY5Y cells. The translocation of phoshatidylserine from the inner leaflet of the plasma membrane to the outer leaflet is observed early in the initiation of apoptosis. This can be observed with Annexin V, a phospholipid binding protein with high affinity for phosphatidylserine. Fig. 3A shows that untreated $N_2A$ cells

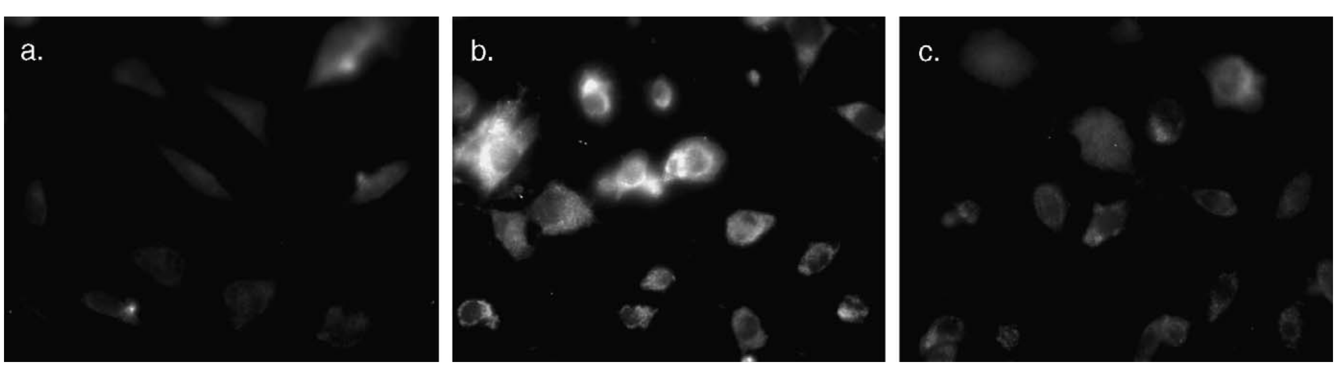


Fig. 2. SS-31 reduced lipid peroxidation caused by *t*BHP. $N_2A$ cells were treated with 1 mM *t*BHP alone, or with 10 nM SS-31, for 3 h. Lipid peroxidation was evaluated by measuring HNE Michael adducts using an anti-HNE antibody. (a) Untreated cells; (b) cells treated with 1 mM *t*BHP for 3 h; (c) cells treated with 1 mM *t*BHP and 10 nM SS-31 for 3 h.

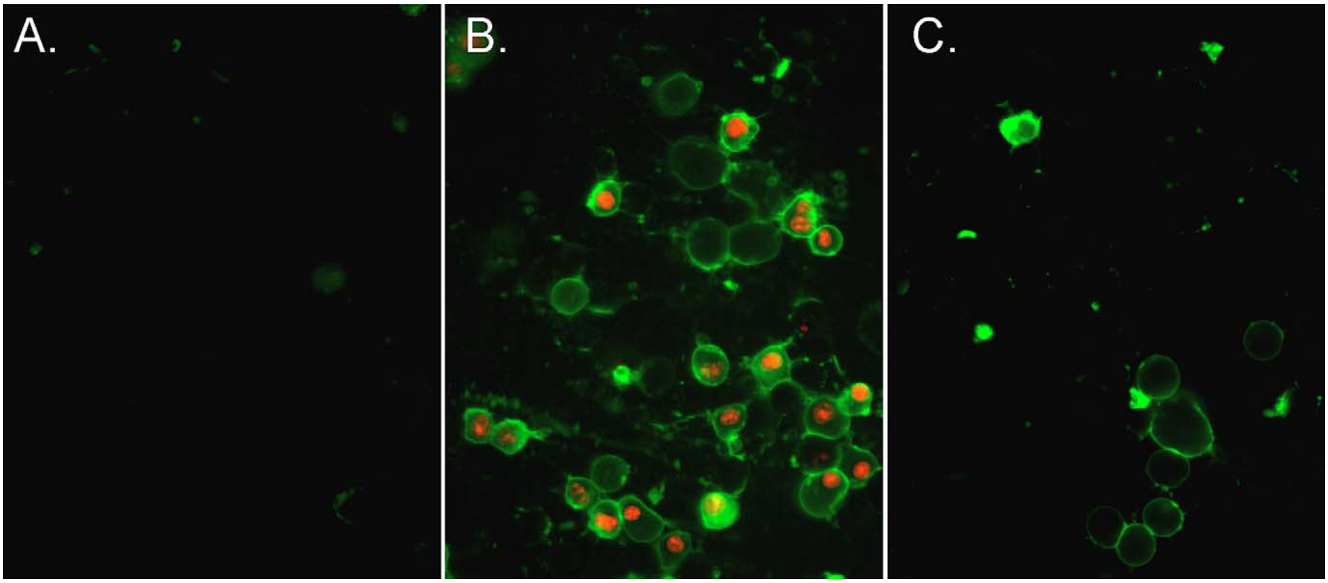


Fig. 3. SS-31 reduced *t*BHP-induced apoptosis as demonstrated by phosphatidylserine translocation. $N_2A$ cells were incubated with 50 μM *t*BHP for 6 h and stained with Annexin V and propidium iodide (PI). (A) Untreated cells showed little Annexin V stain and no PI stain. (B) Cells treated with *t*BHP showed intense Annexin V staining (green) in most cells. Combined staining with Annexin V and PI (red) indicate late apoptotic cells. (C) Concurrent treatment with 1 nM SS-31 resulted in a reduction in Annexin V-positive cells and no PI staining.

showed little to no Annexin V staining (green). Incubation of $N_2A$ cells with 50 μM *t*BHP for 6 h resulted in Annexin V staining on the membranes of most cells (Fig. 3B). Combined staining with Annexin V and propidium iodide (red) showed many late apoptotic cells (Fig. 3B). Concurrent treatment of $N_2A$ cells with 1 nM SS-31 and 50 μM *t*BHP resulted in a reduction in Annexin V-positive cells and no propidium iodide staining (Fig. 3C), suggesting that SS-31 protected against *t*BHP-induced apoptosis.

The morphological appearance of cells treated with *t*BHP was also consistent with apoptosis. $N_2A$ cells incubated with 50 μM *t*BHP for 12 h became rounded and shrunken (Fig. 4A, panel b). Staining with Hoechst 33324 showed increased number of cells with nuclear fragmentation and condensation (Fig. 4A, panel b′). These nuclear changes were abolished by concurrent treatment with 1 nM SS-31 (Fig. 4A, panel c′). The number of apoptotic cells was dose-dependently reduced by concurrent treatment with SS-31 ($P < 0.0001$) (Fig. 4B).

An increased number of cells with condensed nuclei was also observed when SH-SY5Y cells were treated with 25 μM *t*BHP for 24 h, and the number of apoptotic cells was dose-dependently reduced by concurrent treatment with SS-31 ($P < 0.0001$) (Fig. 4C).

### 3.4. SS-31 protected against tBHP-induced caspase activation

Apoptosis induced by *t*BHP has been shown to be caspase-dependent [32,2,33]. Incubation of $N_2A$ cells with 100 μM *t*BHP for 24 h resulted in a significant increase in pan-caspase activity that was dose-dependently prevented by co-incubation with SS-31 ($P < 0.0001$) (Fig. 5A). Caspase-9, in particular, has been shown to be involved in *t*BHP-induced apoptosis [33]. $N_2A$ cells treated with 50 μM *t*BHP for 12 h showed intense staining (red) for caspase-9 activity (Fig. 5B, panel b). Note that cells that show nuclear condensation all showed caspase-9 staining. Concurrent incubation with 1 nM SS-31 reduced the number of cells showing caspase-9 staining (Fig. 5B, panel c).

### 3.5. SS-31 inhibited tBHP-induced increase in intracellular ROS

Intracellular ROS production appears to be an early and critical event in oxidant-induced cytotoxicity [10,8]. Treatment of $N_2A$ cells with 100 μM *t*BHP resulted in rapid increase in intracellular ROS, as measured by DCF fluorescence, over 4 h at 37 °C (Fig. 6A). Concurrent treatment with SS-31 dose-dependently reduced the rate of ROS production, with 1 nM SS-31 effectively reducing ROS production by >50%. The reduction in intracellular ROS was confirmed by fluorescent microscopy with DCF (Fig. 6B). Treatment with $N_2A$ cells with 50 μM *t*BHP caused significant increase in DCF fluorescence (green), and this was significantly reduced by co-incubation with 1 nM SS-31 (Fig. 6C).

### 3.6. SS-31 prevented tBHP-induced mitochondrial depolarization

Opening of the MPT pore and loss of mitochondrial membrane potential have been linked to oxidative cell

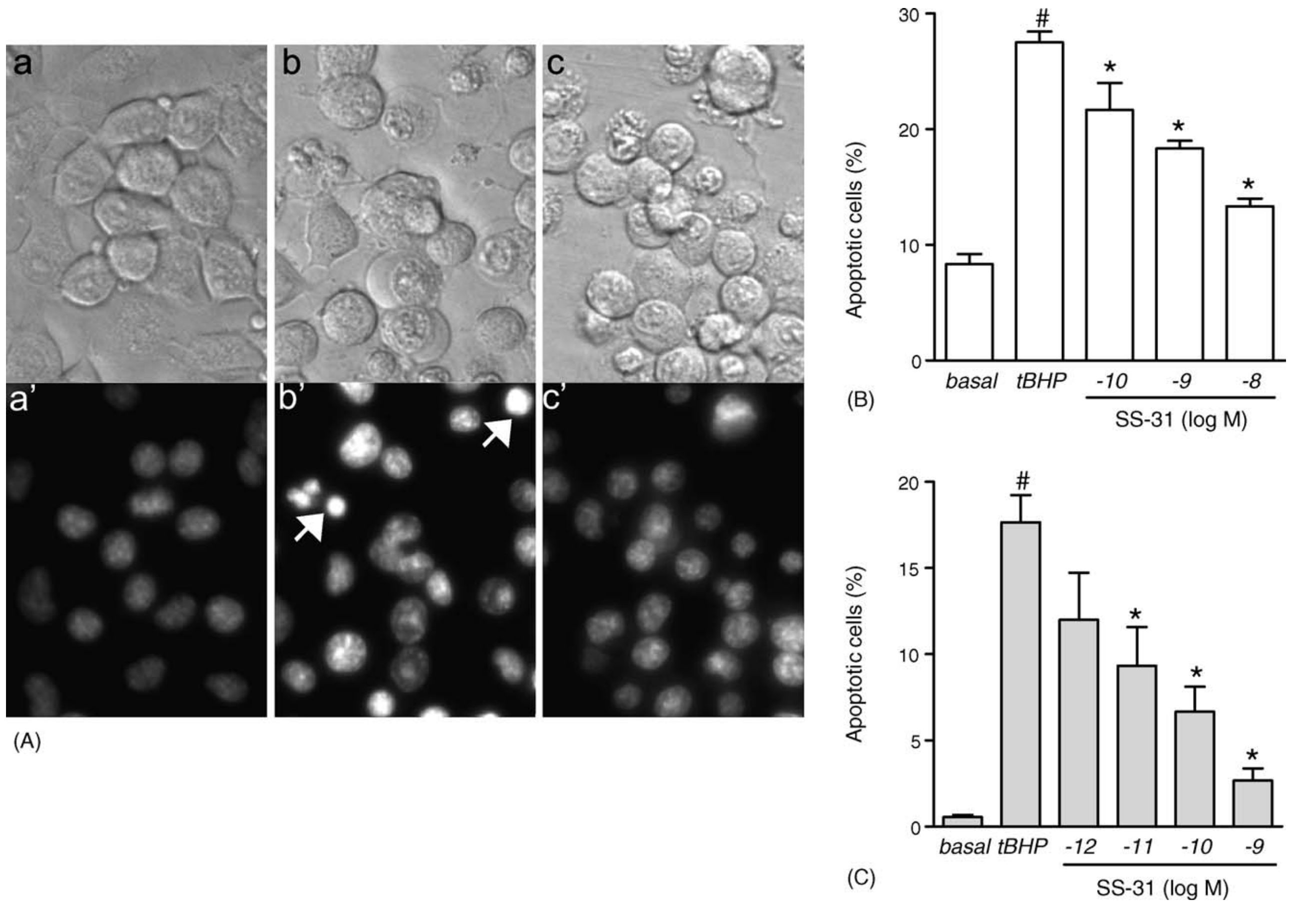


Fig. 4. SS-31 reduced *t*BHP-induced apoptosis as demonstrated by nuclear condensation. (A) $N_2A$ cells were treated with 50 μM *t*BHP alone, or with SS-31, for 12 h. Cells were stained with Hoechst 33342 for 20 min, fixed, and imaged by fluorescent microscopy. (a) Untreated cells show uniformly stained nuclei (a′). (b) Cells treated with *t*BHP were smaller and showed nuclear fragmentation and condensation (b′). (c) Cells treated with *t*BHP and 1 nM SS-31 had less nuclear changes (c′). (B) SS-31 dose-dependently reduced percent of apoptotic cells in $N_2A$ cells. Apoptotic cells were counted using MetaMorph software. $^{\#}P < 0.01$ compared to untreated cells; $^{*}P < 0.01$ compared to *t*BHP alone. (C) SS-31 dose-dependently reduced percent of apoptotic cells in SH-SY5Y cells. SH-SY5Y cells were treated with 25 μM *t*BHP for 24 h. $^{\#}P < 0.01$ compared to untreated cells; $^{*}P < 0.01$ compared to *t*BHP alone.

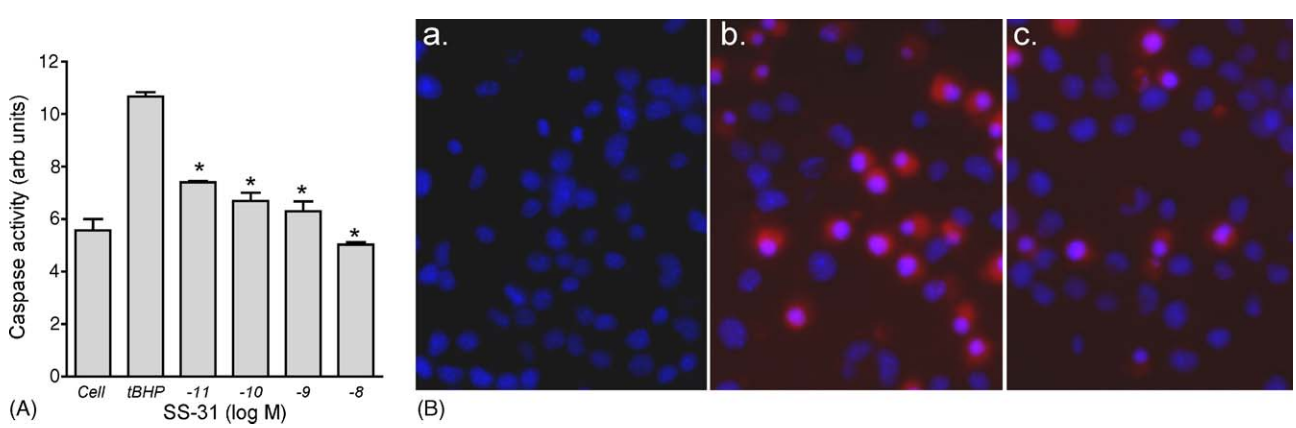


Fig. 5. SS-31 prevented caspase activation in $N_2A$ cells treated with *t*BHP. (A) Incubation of $N_2A$ cells with 100 μM *t*BHP for 24 h resulted in a significant increase in pan-caspase activity that was dose-dependently prevented by co-incubation with SS-31 ($^{*}P < 0.01$ compared to *t*BHP alone). (B) $N_2A$ cells were treated with 50 μM *t*BHP for 12 h and stained with caspase-9 FLICA$^{TM}$ kit containing red fluorescent inhibitor SR-LEHD-FMK and Hoechst 33342. (Panel a) Untreated cells showed no caspase-9 stain and uniformly stained nuclei. (Panel b) Cells treated with *t*BHP showed intense caspase-9 activity (red) in cells that also show condensed nuclei. (Panel c) Cells treated with *t*BHP and 1 nM SS-31 showed fewer caspase-9 positive cells and fewer condensed nuclei.

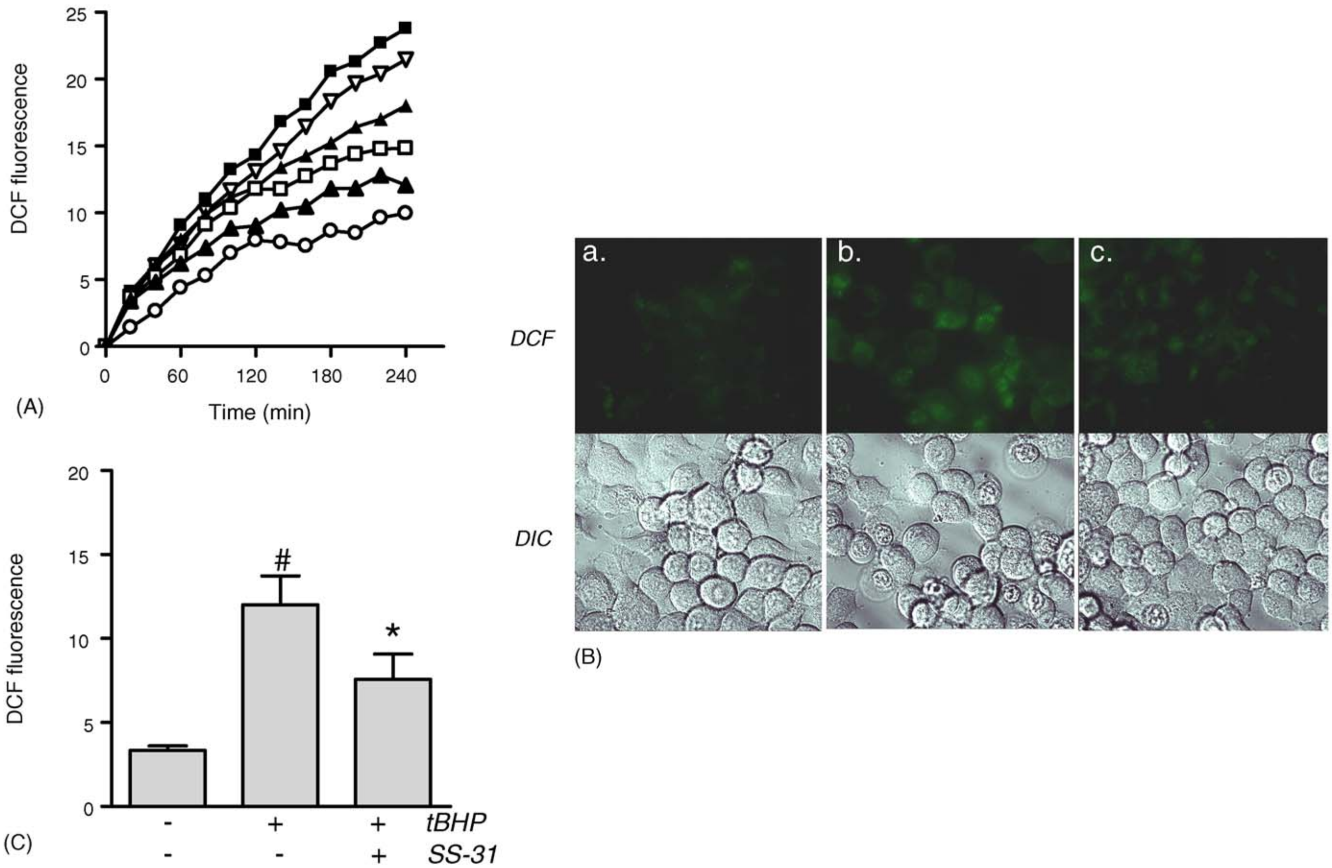


Fig. 6. SS-31 dose-dependently reduced intracellular ROS production in $N_2A$ cells treated with *t*BHP. (A) $N_2A$ cells were loaded with DCFDA, and then exposed to 100 μM *t*BHP alone, or with SS-31. Intracellular ROS was quantified by the formation of fluorescent DCF. Results shown are mean values ($n = 3$). (B) $N_2A$ cells were plated in glass bottom dishes and treated with 50 μM *t*BHP, alone or with 1 nM SS-31, for 6 h. Cells were loaded with DCFDA (10 μM) and imaged by confocal laser scanning microscopy using ex/em of 495/525 nm. (C) Effect of 1 nM SS-31 in reducing intracellular ROS induced by 50 μM *t*BHP ($^{\#}P < 0.001$ compared to untreated cells; $^{*}P < 0.05$ compared to *t*BHP alone).

death caused by *t*BHP [9,10,2]. We therefore investigated whether SS-31 prevents mitochondrial depolarization caused by *t*BHP. Treatment of $N_2A$ cells with 50 μM *t*BHP for 6 h resulted in a dramatic loss of mitochondrial potential. Fluorescence intensity of TMRM (red), a cationic indicator that is taken up into mitochondria in a potential-dependent manner, was significantly lower in cells treated with 50 μM *t*BHP (Fig. 7A; panel b), and this was completely blocked by concurrent treatment with 1 nM SS-31 (Fig. 7A; panel c).

### 3.7. SS-31 prevented loss of mitochondrial function caused by tBHP

Treatment with low doses of *t*BHP (50–100 μM) for 24 h resulted in a significant decrease in mitochondrial function as measured by the MTT assay in both cell lines. Only viable mitochondria containing NADPH dehydrogenase activity are capable of cleaving MTT to the formazan [34]. A 50 μM *t*BHP induced 50% loss of mitochondrial function in $N_2A$ cells (Fig. 7C; $P < 0.01$) and 30% loss of mitochondrial function in SH-SY5Y cells (Fig. 7D; $P < 0.01$). Concurrent treatment with SS-31 dose-dependently reduced *t*BHP-induced mitochondrial toxicity in both $N_2A$ (Fig. 7C; $P < 0.0001$) and SH-SY5Y cells (Fig. 7D; $P < 0.0001$). The non-scavenging peptide, SS-20, did not protect against *t*BHP-induced mitochondrial dysfunction in $N_2A$ cells (Fig. 7C). Treatment of $N_2A$ cells with SS-31 alone had no effect on mitochondrial function (data not shown).

### 3.8. Cellular and mitochondrial uptake of SS-31

We have previously shown that an analog of SS-31, SS-02 (Dmt-D-Arg-Phe-Lys-$NH_2$), readily penetrates SH-SY5Y cells despite a molecular weight of 640 and 3+ net charge [28]. In this study, we examined the cellular uptake of [$^3$H]SS-31 into $N_2A$ cells. [$^3$H]SS-31 was readily taken up into $N_2A$ cells, with steady state conditions achieved by 30 min (Fig. 8A). Based on cell volume of ∼1 μl/$10^6$ cells, the intracellular concentration of SS-31 at steady state can be estimated to be ∼6 times greater than extracellular concentration.

Mitochondrial uptake of [$^3$H]SS-31 was determined in mouse liver mitochondria. Isolated mitochondria were incubated with [$^3$H]SS-31 and 1 μM SS-31 and radio-

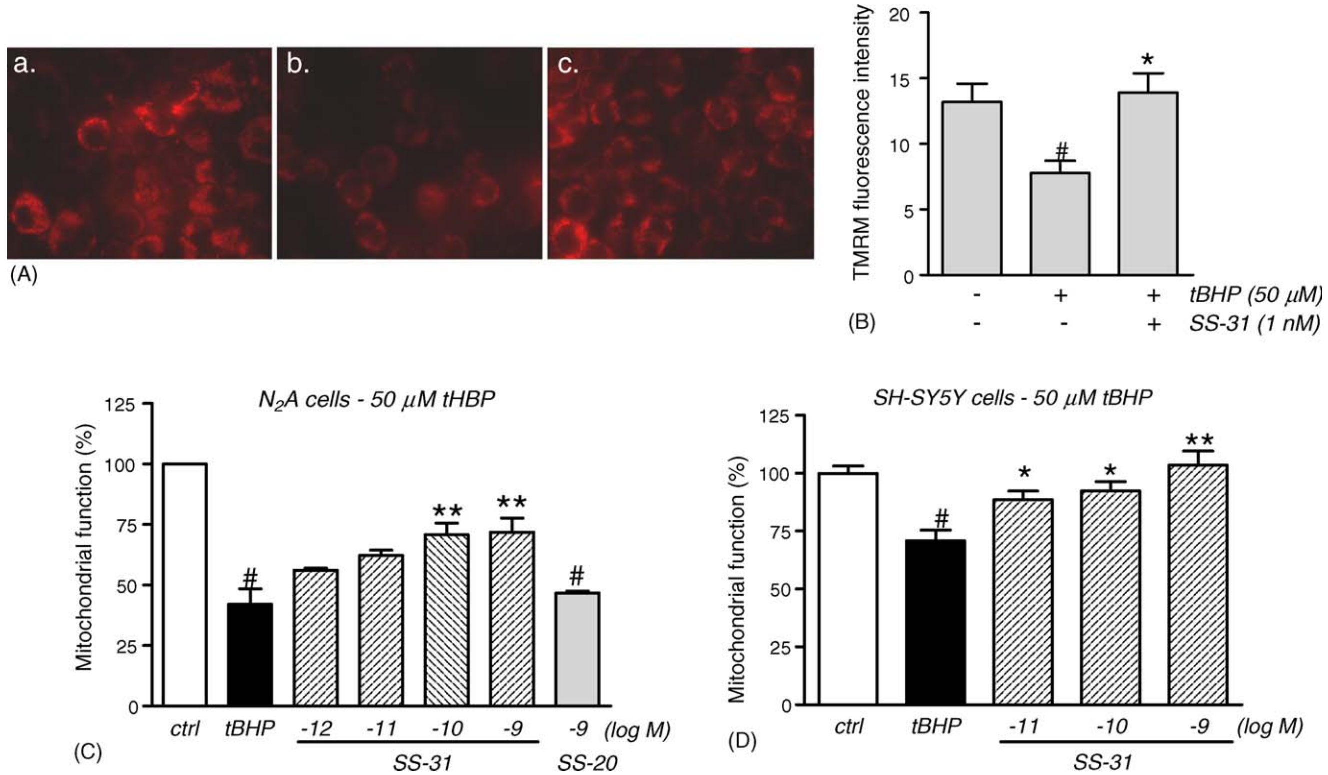


Fig. 7. SS-31 protected against *t*BHP-induced mitochondrial depolarization and viability. (A) $N_2A$ cells were plated in glass bottom dishes and treated with 50 μM *t*BHP, alone or with 1 nM SS-31, for 6 h. Cells were loaded with TMRM (20 nM) and imaged by confocal laser scanning microscopy using ex/em of 552/570 nm. (B) Effect of 1 nM SS-31 in preventing loss of mitochondrial potential induced by 50 μM *t*BHP ($^{\#}P < 0.05$ compared to untreated cells; $^{*}P < 0.05$ compared to *t*BHP alone). (C) SS-31 protected mitochondrial viability in $N_2A$ cells treated with *t*BHP for 24 h. Mitochondrial viability was evaluated using the MTT assay ($^{\#}P < 0.01$ compared to untreated cells; $^{*}P < 0.05$, $^{**}P < 0.01$ compared to *t*BHP alone). (D) SS-31 protected mitochondrial viability in SH-SY5Y cells treated with *t*BHP for 24 h ($^{\#}P < 0.01$ compared to untreated cells; $^{**}P < 0.01$ compared to *t*BHP alone).

activity was determined in the mitochondrial pellet and the supernatant. Uptake of [$^3$H]SS-31 by mitochondria was rapid with maximal levels (~30%) reached before 2 min (Fig. 8B). Radioactivity averaged 67,021 ± 2008 cpm in the mitochondrial pellet, and 128,131 ± 2015 cpm in the supernatant after 10 min incubation ($n = 3$). The uptake of SS-31 was concentration-dependent with no evidence of saturation at concentrations up to 10 μM (Fig. 8C). Uptake of [$^3$H]SS-31 by rat brain mitochondria was even more extensive, with 57.9 ± 0.01% ($n = 3$) of radioactivity found in the mitochondrial pellet after 10 min incubation. Assuming mitochondrial volume of 0.1 μl (~1 μl/mg protein) [35], and incubation volume of 0.5 ml, SS-31 can be estimated to concentrate ~5000-fold in mitochondria.

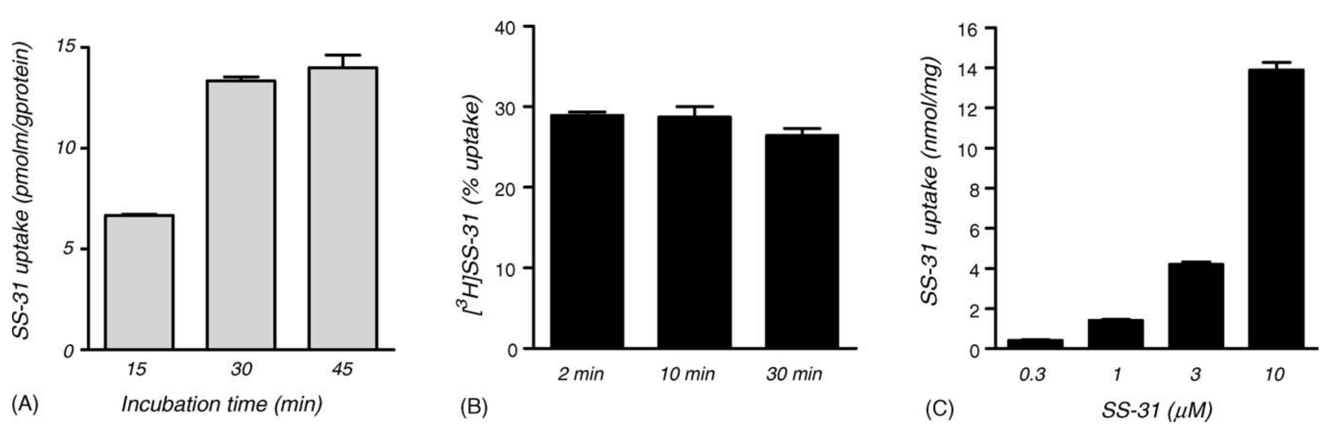


Fig. 8. (A) Cellular uptake of SS-31. $N_2A$ cells ($2 \times 10^5$/well) were incubated with 0.3 ml of [$^3$H]SS-31 and 1 μM SS-31 at 37 °C for 60 min, and radioactivity was determined in the medium and in cell lysate. The reading in medium was subtracted from the reading obtained in cell lysate. (B) Mitochondrial uptake of SS-31. Isolated mouse liver mitochondria were incubated with [$^3$H]SS-31 and 1 μM SS-31 at 37 °C for 2 min, and radioactivity determined in the mitochondrial pellet. (C) Concentration-dependent uptake of SS-31 in isolated mouse liver mitochondria. Each experiment was carried out in triplicate.

## 4. Discussion

Depending on the dose and duration of exposure, cell death caused by *t*BHP can be apoptotic or necrotic [1]. In the present study, 25–50 μM *t*BHP induced apoptosis in $N_2A$ and SH-SY5Y cells as demonstrated by increased number of cells with phosphatidylserine translocation, condensed nuclei, and elevated caspase activity. Co-incubation with SS-31 dose-dependently reduced tBHP-induced apoptosis, with significant reduction observed at 0.1 and 1 nM. Necrosis was observed with $\geq$50 μM *t*BHP, and the release of LDH was also dose-dependently prevented by similar concentrations of SS-31. The cytoprotection provided by SS-31 appears to be due to its antioxidant action because the non-scavenging peptide analog, SS-20, did not protect against *t*BHP-induced cytotoxicity. Although oxidant-induced cell death can be prevented by a number antioxidants, none have been effective at concentrations less than 1 μM [8,36,37].

*t*BHP is cell-permeant and can be readily converted to *tert*-butoxyl radicals via iron-dependent mechanisms which can result in lipid peroxidation. An increase in lipid peroxidation was observed in $N_2A$ cells treated with *t*BHP, but this was prevented by concurrent treatment with as little as 1 nM SS-31. In addition to the formation of butoxyl radicals, *t*BHP promotes intracellular ROS production [10,8,5,7]. Our results show that SS-31, at concentrations that inhibit *t*BHP-induced apoptosis, also prevented intracellular ROS production. Increase in intracellular ROS has been shown to trigger mitochondrial depolarization in hepatocytes and hepatoma cells treated with *t*BHP [9,10]. *t*BHP-induced mitochondrial depolarization can be prevented by MPT inhibitors or antioxidants [10], suggesting that intracellular ROS induces MPT resulting in mitochondrial depolarization. This is supported by the finding that oxidants have been shown to induce MPT in isolated mitochondria [38–41]. In the present study, mitochondrial depolarization resulting from *t*BHP exposure was entirely blocked by co-incubation with 1 nM SS-31, and mitochondrial viability was protected by SS-31 in both neuronal cell lines.

Opening of the MPT pore leads to mitochondrial swelling, rupture of the outer mitochondrial membrane, and release of cyt *c* from the mitochondria to the cytosol where it can activate caspase-9 resulting in apoptosis. Translocation of cytochrome *c* from mitochondria to cytosol, and caspase-9 activation were observed when $N_2A$ cells were treated with 50 μM *t*BHP. Our results therefore suggest that SS-31 inhibits *t*BHP-induced apoptosis by decreasing intracellular ROS production, preventing MPT, and inhibiting caspase-9 activation. Using isolated mouse liver mitochondria, we previously showed that SS-31 can inhibit $Ca^{2+}$-induced MPT and swelling, and reduce cyt *c* release [25]. The inability of SS-20 to protect mitochondrial function is consistent to our previous report that SS-20 was unable to prevent mitochondrial swelling induced by calcium overload [25].

Other antioxidants have been shown to be effective in preventing MPT and cell death caused by *t*BHP, but SS-31 is by far the most potent compound, acting in nM concentrations. Other antioxidants require $>$1 μM to significantly reduce *t*BHP cytotoxicity [10,8,42,43]. The potency of SS-31 may be explained by its cell-permeability and selective concentration in mitochondria. SS-31 was readily taken up into $N_2A$ cells and steady state levels were achieved within 30 min. The robust cellular uptake of such a polar molecule (3+ net charge) might be unexpected, but we have previously reported that an analog of SS-31, SS-02 (Dmt-D-Arg-Phe-Lys-$NH_2$), readily penetrated the cell membrane of several cell types in a passive concentration-dependent manner, including SH-SY5Y cells [28]. Confocal microscopic studies with a fluorescent peptide analog suggested that SS-02 was targeted to mitochondria [25]. Mitochondrial uptake of SS-02 was further confirmed by uptake studies with [$^3$H]SS-02 in isolated mouse liver mitochondria [25]. We now show that [$^3$H]SS-31 is also rapidly taken up into isolated liver and brain mitochondria, with maximal levels achieved within 2 min. Based on the amount of radioactivity in the mitochondrial pellet versus the radioactivity in the incubation buffer, it can be estimated that SS-31 is concentrated ~5000-fold in mitochondria. The 5000-fold concentration in mitochondria can easily account for the extraordinary potency of SS-31 in cell culture studies. The mitochondrial uptake of [$^3$H]SS-31 is almost 10-fold higher than SS-02 (30% versus 4%), and this could account for the greater potency of SS-31 in preventing *t*BHP-induced cytotoxicity compared to SS-02 [25].

The mechanism of uptake for these cationic peptides into mitochondria is not clear. It was initially thought that these 3+ net charge peptides would be targeted to the mitochondrial matrix because of the potential gradient across the inner membrane generated by the extrusion of protons into the intermembrane space. However, the uptake of SS-02 was not dependent on mitochondrial potential and studies with membrane fractionation revealed that [$^3$H]SS-02 was primarily concentrated in the inner membrane rather than in the matrix [25]. The uptake of SS-31 also does not appear to be mediated by specific transporters or receptors because its uptake was not saturable even at concentrations up to 10 μM. The distribution of these peptides in mitochondria is very different from that of mitoQ or mitoVitE [44,45]. The conjugation of a lipophilic cation (TPP+) to coenzyme Q and vitamin E led to their accumulation in the mitochondrial matrix. As a result of the introduction of cations into the matrix, high concentrations of these TPP+ conjugates result in mitochondrial depolarization which may account for the toxicity of these compounds at concentrations $>$10 μM [44]. Exposure of a variety of cell types to SS-31 has not resulted in any cytotoxicity even at concentrations of 1 mM.

By concentrating in the inner mitochondrial membrane, these antioxidant peptides are targeted to the site of ROS production and can therefore protect mitochondria against oxidative damage. As dysfunctional mitochondria can in turn produce more ROS, these mitoprotective peptides can therefore further reduce mitochondrial ROS production. Thus SS-31 can scavenge free radicals as well as protect mitochondria and inhibit ROS production. Besides their unique feature of cell permeability and selective targeting of mitochondria, and lack of toxicity, these peptide antioxidants also possess highly favorable pharmacokinetic profiles, including water solubility, stability, apparent ease in crossing the blood–brain barrier, and relatively long elimination half-lives [46–48]. Mitochondrial dysfunction and oxidative damage are associated with aging and a large number of diseases including ischemia-reperfusion injury, neurodegeneration, cardiovascular diseases and diabetes. Delivery of drugs to mitochondria remains a significant challenge in drug development, and these peptides may provide the design platform that would enable targeted delivery of other drugs to mitochondria.

## Acknowledgements

We thank Dr. Peter Schiller (Clinical Research Institute of Montreal, Montreal, Que., Canada) for providing us with SS-31. [$^3$H]SS-31 was synthesized by Dr. Peter Schiller and Dr. Geza Toth (Isotope Laboratory at the Institute of Biochemistry in the Biological Research Centre, Szeged, Hungary). These studies were supported, in part, by the National Institutes of Health grant numbers DA-08924 and NS-48295.

## References

[1] Haidara K, Morel I, Abalea V, Gascon BM, Denizeau F. Mechanism of *tert*-butylhydroperoxide induced apoptosis in rat hepatocytes: involvement of mitochondria and endoplasmic reticulum. Biochim Biophys Acta 2002;1542:173–85.

[2] Piret JP, Arnould T, Fuks B, Chatelain P, Remacle J, Michiels C. Mitochondria permeability transition-dependent *tert*-butyl hydroperoxide-induced apoptosis in hepatoma HepG2 cells. Biochem Pharmacol 2004;67:611–20.

[3] Rush GF, Alberts D. *tert*-Butyl hydroperoxide metabolism and stimulation of the pentose phosphate pathway in isolated rat hepatocytes. Toxicol Appl Pharmacol 1986;85:324–31.

[4] Masaki N, Kyle ME, Farber JL. *tert*-Butyl hydroperoxide kills cultured hepatocytes by peroxidizing membrane lipids. Arch Biochem Biophys 1989;269:390–9.

[5] Martin C, Martinez R, Navarro R, Ruiz-Sanz JI, Lacort M, Ruiz-Larrea MB. *tert*-Butyl hydroperoxide-induced lipid signaling in hepatocytes: involvement of glutathione and free radicals. Biochem Pharmacol 2001;62:705–12.

[6] Orrenius S, Burkitt MJ, Kass GE, Dypbukt JM, Nicotera P. Calcium ions and oxidative cell injury. Ann Neurol 1992;32(Suppl):S33–42.

[7] Annunziato L, Amoroso S, Pannaccione A, Cataldi M, Pignataro G, D'Alessio A, et al. Apoptosis induced in neuronal cells by oxidative stress: role played by caspases and intracellular calcium ions. Toxicol Lett 2003;139:125–33.

[8] Amoroso S, Gioielli A, Cataldi M, Di RG, Annunziato L. In the neuronal cell line SH-SY5Y, oxidative stress-induced free radical overproduction causes cell death without any participation of intracellular Ca(2+) increase. Biochim Biophys Acta 1999;1452:151–60.

[9] Nieminen AL, Saylor AK, Tesfai SA, Herman B, Lemasters JJ. Contribution of the mitochondrial permeability transition to lethal injury after exposure of hepatocytes to *t*-butylhydroperoxide. Biochem J 1995;307(Pt 1):99–106.

[10] Nieminen AL, Byrne AM, Herman B, Lemasters JJ. Mitochondrial permeability transition in hepatocytes induced by *t*-BuOOH:-NAD(P)H and reactive oxygen species. Am J Physiol 1997;272: C1286–94.

[11] Crompton M, Virji S, Doyle V, Johnson N, Ward JM. The mitochondrial permeability transition pore. Biochem Soc Symp 1999;66:167–79.

[12] Byrne AM, Lemasters JJ, Nieminen AL. Contribution of increased mitochondrial free Ca2+ to the mitochondrial permeability transition induced by *tert*-butylhydroperoxide in rat hepatocytes. Hepatology 1999;29:1523–31.

[13] Kowaltowski AJ, Castilho RF, Vercesi AE. Mitochondrial permeability transition and oxidative stress. FEBS Lett 2001;495:12–5.

[14] Liu X, Kim CN, Yang J, Jemmerson R, Wang X. Induction of apoptotic program in cell-free extracts: requirement for dATP and cytochrome *c*. Cell 1996;86:147–57.

[15] Li P, Nijhawan D, Budihardjo I, Srinivasula SM, Ahmad M, Alnemri ES, et al. Cytochrome *c* and dATP-dependent formation of Apaf-1/caspase-9 complex initiates an apoptotic protease cascade. Cell 1997;91:479–89.

[16] Costantini P, Belzacq AS, Vieira HL, Larochette N, de Pablo MA, Zamzami N, et al. Oxidation of a critical thiol residue of the adenine nucleotide translocator enforces Bcl-2-independent permeability transition pore opening and apoptosis. Oncogene 2000;19:307–14.

[17] Vieira HL, Belzacq AS, Haouzi D, Bernassola F, Cohen I, Jacotot E, et al. The adenine nucleotide translocator: a target of nitric oxide, peroxynitrite, and 4-hydroxynonenal. Oncogene 2001;20:4305–16.

[18] Kanno T, Sato EE, Muranaka S, Fujita H, Fujiwara T, Utsumi T, et al. Oxidative stress underlies the mechanism for Ca(2+)-induced permeability transition of mitochondria. Free Radic Res 2004;38:27–35.

[19] Shidoji Y, Hayashi K, Komura S, Ohishi N, Yagi K. Loss of molecular interaction between cytochrome *c* and cardiolipin due to lipid peroxidation. Biochem Biophys Res Commun 1999;264:343–7.

[20] Murphy MP, Smith RA. Drug delivery to mitochondria: the key to mitochondrial medicine. Adv Drug Deliv Rev 2000;41:235–50.

[21] Inoue M, Sato EF, Nishikawa M, Park AM, Kira Y, Imada I, et al. Mitochondrial generation of reactive oxygen species and its role in aerobic life. Curr Med Chem 2003;10:2495–505.

[22] Maragos WF, Rockich KT, Dean JJ, Young KL. Pre- or post-treatment with the mitochondrial uncoupler 2,4-dinitrophenol attenuates striatal quinolinate lesions.. Brain Res 2003;966:312–6.

[23] Sullivan PG, Rabchevsky AG, Waldmeier PC, Springer JE. Mitochondrial permeability transition in CNS trauma: cause or effect of neuronal cell death? J Neurosci Res 2005;79:231–9.

[24] Sullivan PG, Springer JE, Hall ED, Scheff SW. Mitochondrial uncoupling as a therapeutic target following neuronal injury. J Bioenergy Biomembr 2004;36:353–6.

[25] Zhao K, Zhao GM, Wu D, Soong Y, Birk AV, Schiller PW, et al. Cell-permeable peptide antioxidants targeted to inner mitochondrial membrane inhibit mitochondrial swelling, oxidative cell death, and reperfusion injury. J Biol Chem 2004;279:34682–90.

[26] Zhao GM, Qian X, Schiller PW, Szeto HH. Comparison of [Dmt$^1$]DALDA and DAMGO in binding and G protein activation at mu, delta and kappa opioid receptors. J Pharmacol Exp Ther 2003;307:947–54.

[27] Bedner E, Smolewski P, Amstad P, Darzynkiewicz Z. Activation of caspases measured in situ by binding of fluorochrome-labeled inhibitors of caspases (FLICA): correlation with DNA fragmentation. Exp Cell Res 2000;259:308–13.

[28] Zhao K, Luo G, Zhao GM, Schiller PW, Szeto HH. Transcellular transport of a highly polar 3+ net charge opioid tetrapeptide. J Pharmacol Exp Ther 2003;304:425–32.
[29] Sullivan PG, Rabchevsky AG, Keller JN, Lovell M, Sodhi A, Hart RP, et al. Intrinsic differences in brain and spinal cord mitochondria: implication for therapeutic interventions. J Comp Neurol 2004;474: 524–34.
[30] Mark RJ, Lovell MA, Markesbery WR, Uchida K, Mattson MP. A role for 4-hydroxynonenal, an aldehydic product of lipid peroxidation, in disruption of ion homeostasis and neuronal death induced by amyloid beta-peptide. J Neurochem 1997;68:255–64.
[31] Choudhary S, Zhang W, Zhou F, Campbell GA, Chan LL, Thompson EB, et al. Cellular lipid peroxidation end-products induce apoptosis in human lens epithelial cells. Free Radic Biol Med 2002;32:360–9.
[32] Yang JC, Cortopassi GA. Induction of the mitochondrial permeability transition causes release of the apoptogenic factor cytochrome *c*. Free Radic Biol Med 1998;24:624–31.
[33] Pias EK, Aw TY. Early redox imbalance mediates hydroperoxide-induced apoptosis in mitotic competent undifferentiated PC-12 cells. Cell Death Differ 2002;9:1007–16.
[34] Huet O, Petit JM, Ratinaud MH, Julien R. NADH-dependent dehydrogenase activity estimation by flow cytometric analysis of 3-(4,5-dimethylthiazolyl-2-yl)-2,5-diphenyltetrazolium bromide (MTT) reduction. Cytometry 1992;13:532–9.
[35] Lim KH, Javadov SA, Das M, Clarke SJ, Suleiman MS, Halestrap AP. The effects of ischaemic preconditioning, diazoxide and 5-hydroxydecanoate on rat heart mitochondrial volume and respiration. J Physiol 2002;545:961–74.
[36] Park JE, Yang JH, Yoon SJ, Lee JH, Yang ES, Park JW. Lipid peroxidation-mediated cytotoxicity and DNA damage in U937 cells. Biochimie 2002;84:1199–205.
[37] Huang Z, Senoh Y, Katoh S, Miwa N. Preventive effects of a water-soluble derivative of chroman moiety of Vitamin E on lipid hydroperoxide-induced cell injuries and DNA cleavages through repressions of oxidative stress in the cytoplasm of human keratinocytes. J Cell Biochem 2004;92:425–35.
[38] Kakkar P, Mehrotra S, Viswanathan PN. Interrelation of active oxygen species, membrane damage and altered calcium functions. Mol Cell Biochem 1992;111:11–5.
[39] Aronis A, Komarnitsky R, Shilo S, Tirosh O. Membrane depolarization of isolated rat liver mitochondria attenuates permeability transition pore opening and oxidant production. Antioxid Redox Signal 2002;4:647–54.
[40] Valle VG, Fagian MM, Parentoni LS, Meinicke AR, Vercesi AE. The participation of reactive oxygen species and protein thiols in the mechanism of mitochondrial inner membrane permeabilization by calcium plus prooxidants. Arch Biochem Biophys 1993;307:1–7.
[41] Colell A, Garcia-Ruiz C, Mari M, Fernandez-Checa JC. Mitochondrial permeability transition induced by reactive oxygen species is independent of cholesterol-regulated membrane fluidity. FEBS Lett 2004;560:63–8.
[42] Pong K, Doctrow SR, Huffman K, Adinolfi CA, Baudry M. Attenuation of staurosporine-induced apoptosis, oxidative stress, and mitochondrial dysfunction by synthetic superoxide dismutase and catalase mimetics, in cultured cortical neurons. Exp Neurol 2001;171:84–97.
[43] Aldini G, Carini M, Piccoli A, Rossoni G, Facino RM. Procyanidins from grape seeds protect endothelial cells from peroxynitrite damage and enhance endothelium-dependent relaxation in human artery: new evidences for cardio-protection. Life Sci 2003;73:2883–98.
[44] Kelso GF, Porteous CM, Coulter CV, Hughes G, Porteous WK, Ledgerwood EC, et al. Selective targeting of a redox-active ubiquinone to mitochondria within cells: antioxidant and antiapoptotic properties. J Biol Chem 2001;276:4588–96.
[45] Jauslin ML, Meier T, Smith RA, Murphy MP. Mitochondria-targeted antioxidants protect Friedreich Ataxia fibroblasts from endogenous oxidative stress more effectively than untargeted antioxidants. FASEB J 2003;17:1972–4.
[46] Szeto HH, Clapp JF, Desiderio DM, Schiller PW, Grigoriants OO, Soong Y, et al. In vivo disposition of dermorphin analog (DALDA) in nonpregnant and pregnant sheep. J Pharmacol Exp Ther 1998;284: 61–5.
[47] Szeto HH, Lovelace JL, Fridland G, Soong Y, Fasolo J, Wu D, et al. In vivo pharmacokinetics of selective mu-opioid peptide agonists. J Pharmacol Exp Ther 2001;298:57–61.
[48] Zhao GM, Wu D, Soong Y, Shimoyama M, Berezowska I, Schiller PW, et al. Profound spinal tolerance after repeated exposure to a highly selective mu-opioid peptide agonist: role of delta-opioid receptors. J Pharmacol Exp Ther 2002;302:188–96.